Department of Electrical and Electronic Engineering

Investigation of Gold Nanorod Monomer Biosensors for Label Free Molecule Detection.

A THESIS SUBMITTED TO BRAC University FOR THE DEGREE OF BACHELOR OF SCIENCE IN ELECTRICAL AND ELECTRONIC ENGINEERING.

Rakib Hasan -12221030
Fazle Rabbi - 12121058

Supervised by Avijit Das

CONTENTS

ABSTRACT

Plasmon resonances have attracted a lot of recent research interest for their potential applications, including bio-sensing, sub-wavelength optics, negative refractive index metamaterials and their ability to produce massively enhanced electromagnetic fields. Localized surface plasmon resonances (LSPR) in metallic nanostructure can offer large electromagnetic enhancements and nanometer-scale localization of electric fields. Their resonance wavelength and properties can be tuned by variation of the nanostructure geometry and are sensitive to environmental refractive index.

This thesis contains in depth investigation of gold nanorod monomer biosensors for label free molecule detection. Some core plasmonic properties of gold and its importance in LSPR sensing are analyzed. In addition, LSPR shifts are closely

observed by varying different physical parameters of the biosensor structure. Furthermore, we closely observed the LSPR response by changing the physical environment of the biosensor structure by tuning corresponding refractive indices. Finally, we explored the responsible factors for the sensitivity of bio-proteins and compared our results with theory.

DECLARATION

We declare that no portion of the work referred to in this thesis has been submitted in support of an application for another degree or qualification of this or any other university or other institute of learning.

14th December 2016

Rakib Hasan, 12221030, EEE, BRACU.
Fazle Rabbi, 12121058, EEE, BRACU.

ACKNOWLEDGEMENTS

Our thesis supervisor Mr. Avijit Das (Lecturer of BRAC University, EEE Department) helped us a lot from the beginning to the end. Thank you sir for your support and very specific guideline. Secondly, we thank our Electrical and Electronic Engineering department for providing us this wonderful opportunity to explore this extremely emerging and challenging field of plasmonics. Finally, we are grateful to our small united thesis group.

Chapter-1

INTRODUCTION

1.1) Nanoplasmonics

Nanoplasmonics is an emerging field that studies light–matter interaction interceded by resonant excitations of surface plasmons in metallic nanostructures. It permits the control of the flow of light and its cooperation with matter at the nanoscale (10^{-4} m). A standout amongst the most encouraging qualities of plasmonic resonances is that they occur at frequencies relating to that of typical electronic excitations in matter. This prompts the presence of solid collaborations between localized surface

plasmons and light emitters placed in the vicinity of metals.

The scattering of light by a dielectric particle is an issue that, in spite of being extremely old, shrouds the exceptionally rich field of material science. It was initially treated hypothetically by Lord Rayleigh, who considered the straightforward instance of circles much smaller than the wavelength of light toward the end of the nineteenth century. [1] His exploration prompted the comprehension of numerous marvels identified with light diffusion. For example, in one of his most well known works, [2] he demonstrated that the scattering of light by a weakened gas takes after a ω^4 law, where ω is the angular frequency of the incoming radiation. This implies at high frequencies (blue), light is scattered more efficiently via air particles than at low frequencies (red). This basic law gives an exquisite clarification on the blueness of the sky, the redness of the dusk, or the yellow shade of the sun.

After two decades, a more broad examination, not constrained to

little particles, was performed by Mie. [3] He built up the full diagnostic investigation of light scattering by spherical particles. Extending a plane wave in spherical waves and coordinating the limit conditions on the item surface, Mie was capable to get the scattering and the absorption cross segments of spheres of any size.

Since the work of Mie, the spherical geometry is the main one for which a precise logical hypothesis portraying the scattering of light by particles exists. Barring the utilization of numerical

strategies, the treatment of whatever other shape requires the presentation of various levels of estimate. Subsequently, based on the Rayleigh and Mie approaches, Gans expanded the hypothetical structure to ellipsoidal geometries, illustrating that the optical properties of metal nanoparticles (NPs) depend firmly on their shape. [4] This clarified why the color of a solution containing ellipsoidal NPs changes when the ratio between the particles' axes is varied.

Hypothetical arrangements clarifying the scattering of light by metal NPs have been proposed over a century ago but the characteristic color of metal NPs has been exploited since the days of the Roman Empire. NPs were utilized as colorants in fabrics, recolored glasses, or earthenware production. Clearly, it was most certainly not realized that the starting point of such extraordinary hues was expected to the nearness of small metallic particles, as the length scale included in the scattering of light by NPs (1 nm–1 μm) is numerous requests of size littler than regular human experience (from 1 mm upwards). As an aftereffect of this, the exploration field lost force after Gans' work, to a great extent on account of the inconceivability of building bright nanometric particles in a controlled way.

In the course of recent decades, nonetheless, late remarkable propels in manufacture and portrayal on the nanoscale have offered ascend to a re-established enthusiasm for the scattering properties of metal NPs. Propels in single-molecule spectroscopy, for example, confocal microscopy, [5, 6] dark field microscopy, [7] furthermore, scanning near field optical

microscopy (SNOM), [8, 9, 10, 11] joined with new improvements in very sensitive detectors, counting avalanche photodiodes (APDs) and photomultiplier tubes (PMTs), have permitted us to associate with and study structures on this scale.

The rise of nanophotonics as a productive exploration field over the previous decade has prompted a profound comprehension of electromagnetic phenomena occurring on the nanoscale and to the identification of plasmonic resonances as the key components controlling the optical response of metallic nano-structures.[12, 13, 14, 15, 16, 17, 18, 19, 20] Today, it is outstanding that the communication of light with noble metals, for example, gold or silver, is for the most part determined by the coherent oscillations of the plasmons in the conduction band.[15, 21] In a basic picture, when light experiences a metallic NP, the connection of the electro-attractive field with the electrons in the metal causes them to abandon their equilibrium positions, offering ascend to a surface charge on the nanostructure. The framework then has a tendency to return to its minimum-energy configuration and the electrons attempt to

come back to their balance positions, prompting the formation of charge-density oscillations inside the NP. At the point when the characteristic frequency of these charge oscillations coincides of that of the outer excitation, the response of the metal nanostructure becomes resonant in nature. These are localized surface plasmon resonances (LSPRs). [18]

1.2) Why Nanoplasmonics

One could contend the present increment in enthusiasm for nano plasmonic detecting stages is simply the consistent result of nanotechnology pushing routine SPR detecting toward new wildernesses. In any case, the most essential question that should be addressed is whether this development is justified regardless of the exertion. Inborn advantages of metal nano structure offer conceivable outcomes which is difficult to be met by traditional SPR sensors. Contrasted with SPRs, where the propagating nature of the plasmonic mode guarantees large effective sensing areas, the strong EM field confinement and the localized nature of LSPRs limits minimum sensing area of metal

nano structure to their size. Consolidated with the likelihood of energizing the LSPRs with direct EM illumination, and thus becoming unnecessary use of bulky coupling methodologies, the utilization of metal nano particle offers extremely encouraging open doors for sensor miniaturization and multiplexing. The strong EM field confinement of LSPRs guarantees smaller penetration depths of the evanescent field into the surrounding dielectric. As an immediate result, bio molecules connected to the nano particle surface possess a much bigger division of the evanescent field, raising the desires of excellent sensitivities for the detection of tiny bio molecules in low amounts.

By and large, a nanoplasmonic biosensor comprises of a nanostructured substrate with perfect microfluidics. The LSPR of the nanostructures can be energized by a VIS-NIR light source, while a spectrometer gathers the necessary light. For high nanostructure surface densities, extinction measurements are the most effortless approach to describe the optical properties. For this situation, light is shed on the plasmonic nanostructures and the transmitted light is dissected with a

spectrometer. However, in the point of confinement of single molecule detecting, a much higher complexity is required between the excitation light and the light consumed by the nanoparticles. In those cases, scattering measurements are favored. These high signal-to-background levels can be accomplished by dark field (DF) microscopy or total internal reflection (TIR) spectroscopy. As the span of the particles is diminished, the scattering cross segment becomes smaller and absorption becomes dominant, making extinction measurements more desirable. In DF microscopy (transmission design) a DF condenser is utilized to focus a hollow – high numerical aperture – cone on the nanostructured substrate. At that point, the scattered light scattered by the nanostructures can be gathered by a magnifying lens objective with a lower numerical gap. Interestingly, in TIR microscopy, the LSPR is energized in a crystal coupled TIR design, subsequently likewise utilizing a magnifying lens target to gather the scattered light, yet for this situation, with no limitation on its numerical aperture. Nanostructured substrates utilized in the nanoplasmonic biosensors can be isolated based on top-down or bottom up

fabrication methodologies. While the former group depends on lithographical designing systems, the last one depends on chemically synthesized colloidal nanoparticles that are further kept on substrates. Thus, we just call attention to the nuts and bolts of both manufacture ideas. For a more point by point and broad data on the creation of nanoplasmonic structures, we allude to the survey by Jones et al. [30]. The current variety and extraordinary optical properties of synthesized nanoparticles can be credited to extraordinary advances in nanotechnology, giving analysts the vital chemistry methods that empower exact geometrical nanoparticle designing. In such manner, next to spheres [31], rods [32, 33, 34], plates [35], triangles [36, 37], (bi)pyramids [38, 39, 40], cubes [41, 42], tubes [43], stars [44] or prisms [45], also hybrid and alloy nanoparticles have been fabricated [46], such as for example core-shell particles [47, 48, 49, 50], nanoflowers [51] or nanorice [52].

In all cases, the nature of colloidal nanoparticles imposes downsides on their utilization as biosensors in arrangement. Changes in the ionic quality, pH or buffer temperature, can

prompt the molecule precipitation. Moreover, surface bio functionalization conventions can screen or change the charge conveyance yielding a break of the colloidal balance. To keep away from these challenges, connection of the colloidal nanostructures to a strong backing can be the best option or even an essential. An extra advantage is its similarity with microfluidics for in-flow detecting assays. To this end, diverse approaches have been created that go for appending the colloidal nanoparticles to already functionalized surfaces through either covalent or electrostatic linkage procedures. Thiol-or amino-adjusted glass surfaces can firmly connect gold nanoparticles to the surface, albeit at times this functionalization step can be particularly dubious with particles that require a stabilizer layer on the surface to maintain a strategic distance from collection, as on account of nanorods, nanoplates or other sort of structures [78, 79]. These surface alterations as a rule impede a proficient and reproducible scope of the strong backing. While trying to beat this issue, extra strides are regularly required including the exchange of this defensive layer

with other functionalized mixes (i.e. PEGylated mixes, thiolated mixes with carboxylic corrosive, biotin, and so on.).

This progression therefore allows for binding to appropriately modified surfaces (amino-, thiol-, avidin-modified or opposite charged surfaces so that electrostatic cooperations happen [80, 53, 54]). An attractive option comprises of straightforwardly developing the nanostructure on the substrate [55]. The surface thickness of immobilized nanoparticles can be controlled by improving parameters, for example, the grouping of the colloidal nanoparticle suspension, the hatching time, or the temperature, making it conceivable to acquire exceedingly thick or exceptionally meager surface focuses. For scanty thickness, between molecule segregation gets to be conceivable, empowering the otherworldly observing of a solitary nanostructure. It ought to be noticed that all these immobilization procedures prompt an arbitrary nanoparticle surface dispersion, yielding low control of both position and introduction. This issue can be overcome via doing a past requested functionalization of the substrate, for case, via

painstakingly adjusting the surface at particular positions that results in an arrayed-based distribution.

The most common top-down creation approaches incorporate routine lithography, for example, photograph lithography, electron beam lithography (EBL) or focused ion beam lithography (FIB), taking into consideration the development of varieties of nanometric structures with very much characterized shapes and sizes [81]. Albeit broadly utilized, these systems are moderate and high-cost, and in spite of high levels of resolution, typically limit the patterning area to only a few μm^2 . On the other hand, conventional photo lithography allows faster, parallel and huge scale manufacture at the expense of lower resolution. An alternate approach for extensive scale and ease making of plasmonic nanostructures is offered by colloidal lithography systems, for example, nanospheres lithography (NSL) [56, 57, 58], or hole-mask colloidal lithography (HCL) [59]. In both strategies, the self-assembled layer of nanospheres onto the substrate is utilized as a conciliatory cover for the era of nanostructured substrates. With NSL, rendershighly requested

designing, while HCL, described by short-run requested varieties of nanostructures, offers more adaptability regarding molecule geometry. Another manufacturing system that currently gets much consideration is nanoimprint lithography. This method depends on the utilization of reusable ace stamps, which can be either hard (unbending) [60], or delicate (elastomeric) [61], that are utilized to engraving or exchange predefined designs onto any fancied substrate. These examples are regularly utilized as a cover for progressive manufacture steps. Because of the reusability of the ace stamps, and even their tunability on account of delicate stamps [62], nano imprint lithography is viewed as an ease system with potential for high throughput manufacture of sub-micron organized substrates. Utilizing this manufacture strategy, extensive nano-designed zones of vaults [63], pits [64], gaps [65], and dots/disks [66, 67, 68] have been reported. An alternate approach is offered by nano stencil lithography. In light of shadow cover testimony, and having the extra advantage of not requiring any oppose handling, heating, or dissolvable utilize, this system manufactures thick nanostructured substrates with high

determination [69], for example, nanodots [70], or nanorods [71], and can even be stretched out for the production of nanoplasmonic structures on adaptable substrates [72, 73]. Alongside these previously mentioned approaches, other top-down techniques that merit specifying incorporate the utilization of permeable alumina formats for the production of vertical nanorods [74] and nanotubes [75], the immediate seed-mediated growth of nanoplates straightforwardly on top of surfaces [82], the utilization of interference lithography [76], or the fabrication of nanoparticle bunch clusters utilizing a hybrid top-down/bottom-up approach [77].

1.3) Nanoplasmonic Sensing

Nanoplasmonic sensing deals with the interaction of light with metallic substances at the nanoscale, commonly in almost 100 nm size extent. This interaction with light summons the direct photon-induced resonant collective oscillation of valence electrons, built up when the frequency of photons matches the natural frequency of the metal electrons wavering against the

re-establishing force of positive nuclei. Such LSPRs are portrayed by a large amplification of the electric field close to the molecule surface and for the most part, field rot lengths littler than the wavelength of the exciting light in free space. Because of the substantial field improvement offered, physical procedures that are delicate to the electric field experience amplification [22, 23, 24].

Nanoplasmonic detection has broadened into an experimental platform for investigations of biomolecular interactions and for biosensors. Enlivened by this success, in later years, nanoplasmonic detection methodologies have been adjusted and custom fitted effectively to probe functional nanomaterials and catalysts in situ and in real time. An expanding number of these studies concentrate on utilizing the LSPR as a test device to ponder a procedure of enthusiasm for a nanomaterial. The key resources of nanoplasmonic sensing here are its remote readout, non-intrusive nature, single molecule analysis capacity, convenience and, perhaps above all, unmatched adaptability as

far as similarity with every material sort (particles and thin or thick layers, conductive or insulating) are distinguished.

There are two generic experimental strategies: Direct Nanoplasmonic Sensing and Indirect Nanoplasmonic Sensing. In a direct nanoplasmonic detection test the plasmonic nanoparticles are active and at the same time constitute the sensor and the concentrated nano-element. In an indirect nanoplasmonic detection test the plasmonic nanoparticles are inert and adjacent to the material of interest to test a procedure occurring in/on this material.

1.4) Overview of the Thesis

In this thesis, we have investigated gold nanorod monomer biosensors for label free molecule detection. In chapter-1, we provided a short overview of nanoplasmonics and its importance for biosensing applications. In chapter-2, we have reviewed

localized surface plasmon resonance in brief and explained some fundamental theories like Lorentz Model, Drude Model, Mie Theory, and Gans Theory. These theories play vital role in modeling and analysis of gold nanorod, bio-proteins, and their interaction with light. Then in chapter-3, we've analyzed some core plasmonic properties of gold and its importance in LSPR sensing. After that we have explained our proposed biosensor structure and described different parts in chapter-4. Chapter-5 is all about the basics of Finite Difference Time Domain (FDTD) simulation where we have explained different aspects of material modeling, biomolecule modeling, necessary boundary conditions, optical sources, and the core formula to calculate power absorption by the proposed biosensor structure. In chapter-6, we have analyzed our simulations and results in detail. We investigated LSPR responses for physical parameter and environment variation of the proposed biosensor structure. Then we concluded chapter-6 by observing the sensitivity of various bio-proteins and explained the core factors responsible for their various characteristics in terms of sensitivity. Finally, in chapter-7, we illustrated future works of this extremely

emerging field of nanoplasmonics and the applications of gold nanorod monomer biosensors for label free molecule detection.

Chapter-2
LOCALIZED SURFACE PLASMON RESONANCE (LSPR)

2.1) Difference between Bulk Plasmon and Localized Plasmon Resonance

The differences is related to the origin of the both phenomena. The origin of localized surface plasmon is the collective oscillation of the electrons at the metal NP's surface, whereas the bulk plasmons is a result of the oscillation of the electrons at the bulk materials. Surface plasmon (in the case of metal nanoparticles) can be excited by barely visible light (for the

overwhelming majorities of noble metal). Bulk plasmons can not be excited by visible light, but rather with a beam of electrons.

2.2) Microscopic Response of the Medium

Metals, for example, gold and silver that are appropriate for plasmonic applications are all around characterized by the Drude Model. Here, the metals comprise of fixed ion cores, encompassed by freely moving conduction electrons. The electrons don't interact with each other, however once in a while, collide instantaneously and elastically with the ion cores. The Drude Model can be derived as a special case of the Lorentz Model of the optical polarisability.

2.2.1) Lorentz Model and Drude Model

The Lorentz Model of the optical polarisability [25] regards a medium as an accumulation of classical driven damped

harmonic oscillators. For an oscillator of mass m, natural frequency ω_0 and damping coefficient λ displaced from equilibrium a distance r by force F,

$$F = m\left(\frac{d^2r}{dt^2} + \lambda\frac{dr}{dt} + \omega_0{}^2 r\right) = -eE$$

For our case the displacing force is created by an electric field E, and follows up on electron charge e. Utilizing complex notation for E and r oscillating at a single frequency ω with time reliance contained in a $e^{-i\omega t}$ factor, and substituting m by the electron effective mass m* we find

$$r = \frac{-eE}{m^*(-\omega^2 - i\lambda\omega + \omega_0{}^2)}$$

The complex dipole moment p induced by the charge separation r is p = -er. The linear polarisability α is defined as $p = \alpha E$. Here,

$$\alpha = \frac{e^2}{m^*(-\omega^2 - i\lambda\omega + \omega_0{}^2)}$$

The macroscopic polarisation of a medium P is linked to its dielectric function by $\varepsilon(\omega) = 1 + \frac{P}{\varepsilon_0 E}$. Assuming that oscillators are non-interacting, we can simply sum all the individual microscopic polarizabilities to find P. So for n electrons, $P = n\alpha E$ and

$$\varepsilon(\omega) = 1 + \frac{ne^2}{m^*\varepsilon_0(-\omega^2 - i\lambda\omega + \omega_0{}^2)} \quad \textbf{(1)}$$

Drude model is simply a special case of the above. In the Drude model, the delocalised conduction electrons move without any restoring force, in other words, $\omega_0 = 0$. We then have

$$\varepsilon(\omega) = 1 - \frac{ne^2}{m^*\varepsilon_0(\omega^2 + i\lambda\omega)} \quad \textbf{(2)}$$

The factor $\frac{ne^2}{m^*\varepsilon_0}$ multiplying the second term on the right hand side has units of s^{-2} , and its square root represents the the bulk plasma frequency of the metal, ω_p .

$$\omega_p = \sqrt{\frac{ne^2}{m^* \varepsilon_0}} \quad \textbf{(3)}$$

We therefore have a frequency dependent dielectric function, $\varepsilon(\omega)$.

$$\varepsilon(\omega) = 1 - \frac{{\omega_p}^2}{\omega^2 + i\lambda\omega} \quad \textbf{(4)}$$

The effect of inter-band transitions can be roughly accounted for by introducing a factor ε_{int}.

$$\varepsilon(\omega) = \varepsilon_{int} - \frac{{\omega_p}^2}{\omega^2 + i\lambda\omega}$$

However the Drude model will fail close to the inter-band transition

2.3) Mie Theory

'Mie Theory' empowers exact assessment of extinction, scattered fields and enhancement factors, yet can be exceptionally cumbersome[25, 26]. The hypothesis accepts a spherical morphology, that the particle and encompassing medium can each be depicted by one dielectric function, and that there is a sharp discontinuity in electron density at the particle surface[27]. For a metal sphere of dielectric function $\varepsilon_M(\omega)$ in a dielectric medium of dielectric constant ε_D in a constant semi static external field of magnitude $E_{incident}$, the inward field of the sphere is given by[25, 28]

$$E_{internal} = \left(\frac{3\varepsilon_D}{\varepsilon_M(\omega) + 2\varepsilon_D}\right) E_{incident} \quad \textbf{(5)}$$

Accepting that the electric potential, φ (where $E_{incident} = -\nabla\varphi$) and the typical component of the electric displacement are both continuous at the sphere surface as our boundary conditions, the

general polarisability of the nanosphere can be computed by solving Laplace's equation, $\nabla^2\varphi = 0$, giving

$$a = 4\pi\varepsilon_0 r^3 \left(\frac{\varepsilon_M - \varepsilon_D}{\varepsilon_M + 2\varepsilon_D}\right) \quad \mathbf{(6)}$$

for a sphere of radius r.

From (5) and (6) we see that, for a metal with small damping, when $\varepsilon_M \approx -2\varepsilon_D$ the polarisability will be tremendous and the field inside the nanoparticle will be significantly amplified. For a theoretical perfect Drude metal, the amplification factor would tend to endlessness. It is the damping $(\mathrm{Im}(\varepsilon_M(\omega)))$ which obliges the amplitude and expands the resonances. The resonance wavelength relies on the frequency dependent dielectric function $\varepsilon_M(\omega)$ of the metal and additionally of the environment. Like SPP resonances, this sensitivity to the dielectric constant/refractive index of the environment is the premise of LSPR bio-detecting systems. For excitation frequencies fundamentally bigger than the dipolar surface

plasmon resonance of the particle the deviation between nanoparticle and thin film behaviour diminishes, as other effects such as inter-band transitions begin to dominate the optical properties[29]. The resonances of sub-wavelength nanostructures depend firmly on the morphology of the structures, and explanatory arrangements of Maxwell's conditions exist for basic geometric shapes. More muddled structures are still impossible to analyze analytically. In these cases, finite element computer simulation can be utilized to anticipate the resonances.

2.4) Gans Theory

Gans hypothesis is the expansion of Mie hypothesis for the instance of spheroidal particles. It gives the dispersing qualities of both oblate and prolate spheroidal particles much littler than the excitation wavelength. Since it is a solution of the Maxwell equations it ought to in fact not be known as a hypothesis.

In Gans hypothesis, the absorption depends on aspect ratio of the particles only. This reliance is presented through polarization or shape factors related to the three dimensions of the particle. For the instance of spheroids, this diminishes to just two distinct factors since the particle is rotational symmetric around one axis. [83]

The absorption coefficient,

$$\sigma_{abs} = \frac{2\pi N V \varepsilon_m}{3\lambda} \sum_{j=A}^{C} \frac{(1/P_j^{\,2})\varepsilon_2}{\left(\varepsilon_1 + \frac{1-P_j}{P_j}\varepsilon_m\right)^2 + \varepsilon_2^{\,2}} \quad \textbf{(7)}$$

Where N = number of particles per unit volume,

V = average volume per particle,

NV = total volume of all particles,

$n^2 \simeq \varepsilon_m$ = dielectric constant of the medium,

λ = absorbed wavelength,

P_j = depolarization or shape factor,

$(\varepsilon_1 + i\varepsilon_2) = \varepsilon$ = complex dielectric function of prolate spheroid.

P_j relates the plasmon excitation to the aspect ratio of the particle for the 3 axes, $j = A,\ B,\ C$ with lengths $L_a,\ L_b,\ and\ L_c.$

Where $L_a > L_b = L_c,$

$R = L_a / L_b\,,$

$P_A = \frac{1-e^2}{e^2}\left(\frac{1}{2e} ln\left(\frac{1+e}{1-e}\right) - 1\right),$

$P_B = P_C = \frac{1-P_A}{2}\,,$

$e = \sqrt{1 - 1/R^2}\,.$

The position of longitudinal absorption peak is strongly dependent on R and ε_m . The transversal plasmon mode is also dependent on R and ε_m but the effect is not significant enough. σ_{abs} increases slightly with increasing R and the increment of σ_{abs} is more significant with higher value

Chapter-3
OPTICAL PROPERTIES OF GOLD

3.1) Noble Plasmonic Metal - Gold

Gold's high conductivity and chemical stability are its most advantageous properties. However, gold has an interband transition in the visible part of the spectrum at around 470 nm and several more in the ultraviolet region at around 325 nm. [84] For these interband transitions, gold is used for plasmonic resonances of wavelength > 600 nm. Damping is smaller in this region and gold much more closely resembles an ideal Drude metal.

The electronic transition in a solid are more directly related to the complex dielectric constant, $\bar{\varepsilon} = \varepsilon_1 + i\varepsilon_2$ instead of complex refractive index, $\bar{n} = n + ik$. Here, $\bar{\varepsilon} = \bar{n}^2$. So, $\varepsilon_1 = n^2 - k^2$ and $\varepsilon_2 = 2nk$. The optical constants n and k are determined by inverting the normal-incidence reflection and transmission functions, R_0 *and* T_0. [85]

Data analysis for plasmonic property of gold was done in terms of the complex refractive index, $\bar{n} = n + ik$. Then we've evaluated ε_1 and ε_2 from n and k and plotted ε_1 and ε_2 with respect to photon energy (eV). The graphs are given below:

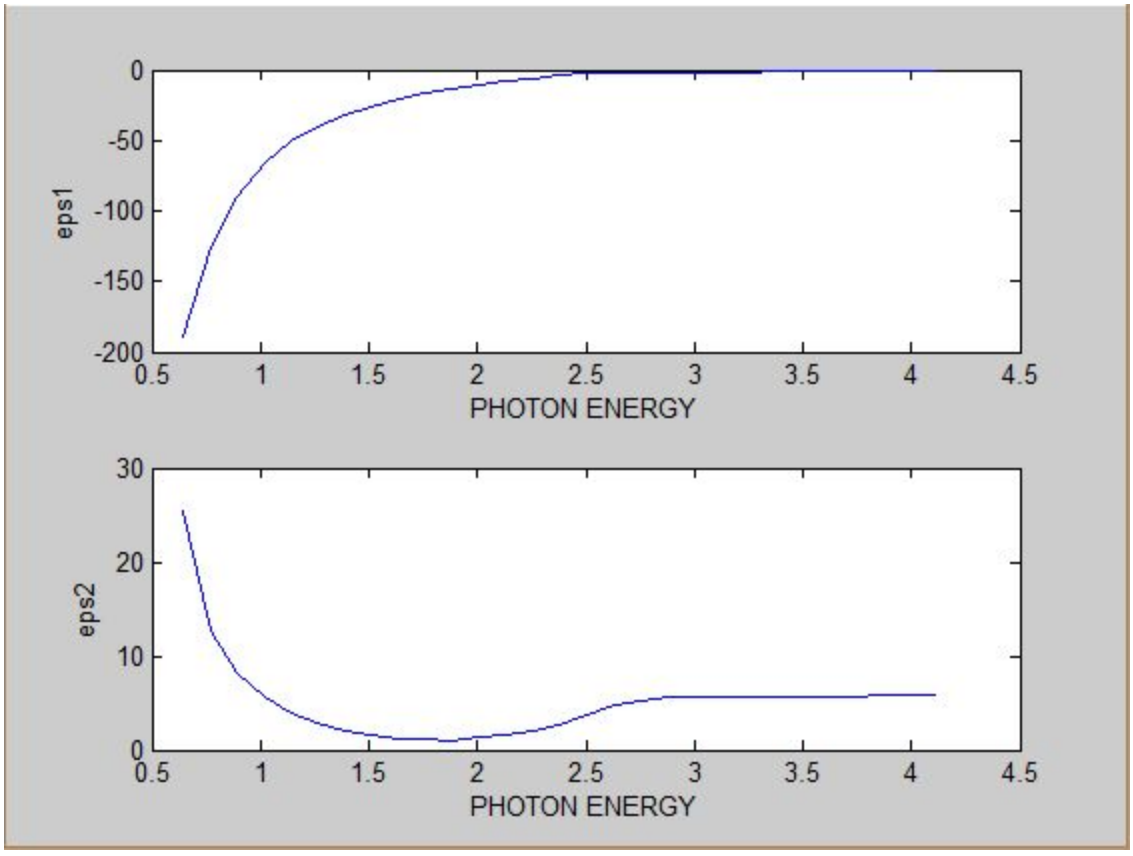

Fig.1. ε_1 , ε_2 vs eV Graph

Chapter-4

GOLD NANOROD MONOMER BIOSENSOR

4.1) Proposed Biosensor

We have constructed our biosensor utilizing gold nanorod monomer, bio-protein, biotin layer (to attach the nanorod with protein molecule), and glass substrate. The proposed biosensor diagram is shown below.

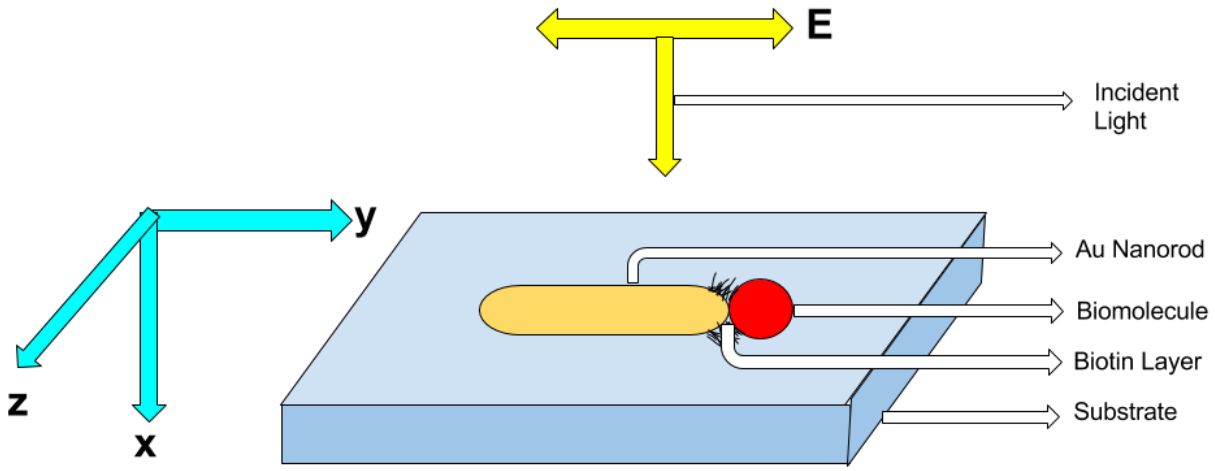

Fig.2. Proposed biosensor diagram.

We varied the protein molecule to check sensitivity of different biomolecules with the variation of size, shape, and refractive index. Then we varied the substrate to check the LSPR shift with the variation of physical environment. We used TFSF source as incident light (E) to form localized surface plasmon resonance with the variation of frequency of light.

Chapter-5

FDTD SIMULATION

5.1) Introduction

The finite difference time domain (FDTD) is an application of Maxwell's time dependent curl equation to solve the temporal variation of Electromagnetic (EM) waves within a finite space that contains a target of arbitrary shape and has recently become the most effective method to solve Maxwell's equations for complex geometries. FDTD offers users an unique insight into time and space solution. In addition, FDTD can also be used to obtain the frequency solution by exploiting Fourier Transforms.

In the FDTD technique, Maxwell's curl equations are discretized by using finite difference approximation in both time and and space that are easy to program and are accurate. To achieve high accuracy to realize the spatial derivatives involved, the algorithm positions the components of the electric field

about a unit cell of the lattice that constitutes the FDTD computational domain.

5.2) Material Modeling

Material modeling is one of the most important parts of FDTD simulation workflow. The geometry of a structure is constructed by different materials. Each component material must be properly modeled to account for their dispersive nature. In our thesis, the material modeling is done via experimental values of complex refractive index measured at sampled wavelength values. For intermediate arbitrary wavelength, interpolated values have been used. Gold (Au) exhibits the metal layers in our proposed biosensor structure. Modeling of metals is very critical in FDTD analysis as their parameters vary substantially in different data sets. In our work, data obtained from Johnson and Christy have been used to model Au. Chaotropic agents has been considered as the buffer medium. For our simulation, the refractive indices of chaotropic agents have been chosen as

1.3448, 1.3668, and 1.3848. To model the substrate we have taken frequency dependent refractive index (RI) values which also has been varied from hydrophilic SiO_2 to hydrophobic Teflon-AF to show the substrate effect.

5.3) Biomolecule Modeling

Modeling of biomolecule is another important factor of FDTD simulation. The biosensing performance of the proposed structure largely depends on how the protein samples are modeled. It is required to model the protein samples according to their original sizes and shapes otherwise practical results can not be predicted from FDTD simulations. In our study we have taken protein samples with significant differences in their tertiary sizes ranging from 14.3 kDa to 390 kDa. The adsorption of chicken egg white lysozyme (Lys), human serum albumin (HSA), human γ - immunoglobulin (IgG), adenomatous polyposis coli (APC) and human fibrinogen (Fb) have been modeled on glass substrate adjusted with the gold nanorod

monomer. Characteristic differences of these proteins have been highlighted through shapes refractive indices (RI). The sizes, shapes, and RI values of these modeled biosamples are shown in the following table:

Protein	Dimension (nm)	Mass (kDa)	Refractive Index
HSA	$8 \times 7 \times 4$	66.4	1.45
Fb	$12 \times 3 \times 6$	390	1.39
APC	$4.8 \times 4.5 \times 4.3$	275	1.46
IgG	$4 \times 3.6 \times 3$	148	1.42
Lys	$1.9 \times 1.9 \times 1.9$	14.3	1.495

A 0.5 nm biotin layer has been added in the gap region between the nanorod and the protein. The RI value of biotin layer has been considered as 1.45 . With the proposed structure incident at transverse magnetic (TM) and transverse electric (TE) polarized

light, the SPR Shifts for these bio-proteins have been calculated to find out their molecular sensitivity.

5.4) Boundary Conditions

Depending on the purpose of optical simulation some kind of boundary conditions must be applied. Boundary conditions are nothing more than mathematical description that defines how field quantities should behave as they reach the edge of the simulation region. For simulation purpose, mainly two sets of boundary conditions were used. One is perfectly matched layer (PML) and the other is periodic boundary condition.

5.4.1) Perfectly Matched Layers

Perfectly matched layer (PML) defines the boundary condition that ensure that outgoing radiations that reach the edge of the simulation boundary will die out at the boundary without

reflecting back into the simulation region to interfere with the field inside. An ideal PML boundary will absorb all of the electromagnetic field incident on it. However, it does not happen in real PML condition. Depending on the number of layers, a real PML can only approximate an ideal PML boundary with different accuracy. While the absorption is maximum in case of normal incidence, oblique incidence can result insignificant reflection back into the simulation region. So number of layers must be chosen carefully in a direction of interest to simulate the practical scenario as accurately as possible. In our simulation we have taken 12 layers to provide consistency with the experimental results. Also this boundary condition works best if the structure is extended through the simulation boundary. PML boundary is used to simulate and study the behavior of an isolated structure. If a structure is surrounded by a simulation region with PML boundary condition imposed on every side, it can be assumed to be isolated. The only excitation source will be the source placed within the boundary. The electromagnetic field profile observed after simulating will be only due to the perturbation of that structure alone.

5.4.2) Periodic

Periodic boundary condition is mainly used with broadband wave source. Unlike PML, field does not exactly die out at the edge of the simulation region. Rather it assumes that similar structure continues in that direction. FDTD simulator then takes into account of presence of similar structure in the direction and calculates the field profile accordingly. It is possible to impose different boundary conditions on different directions.

5.5) Optical Sources

Optical source is very important for proper optical simulation of a given structure. In our thesis, we have utilized Total Field Scattered Field (TFSF) source which is particularly used to understand the behavior of scattering and absorption from small particle. It is also convenient to properly evaluate the electric field enhancement at the edges of nanorod structure. A TFSF

source is modeled in such a way that it splits the simulation region in two different regions.

- Total field region: contains the total field,
- Scattered field region: only contains the scattered field.

Within the boundary of the source it is a plane wave that propagates with a wave vector normal to its surface incidence. At the edge of the boundary the absorbed field is subtracted from the total field leaving only the scattering field to propagate outside. When it acts as a plane wave it can be defined to have a fixed polarization. Depending on the angle of polarization it will give TF (for angle 90^0) or TM (for angle 0^0) wave propagation in 3D simulation.

5.6) Power Absorption

Spatial power absorption in the structure was calculated using the formula,

$$P_{abs} = \frac{1}{2} \times \omega \times Imag(\varepsilon) \times |E|^2$$

Where ω = frequency of incident light,

ε = permittivity of the material at the point at which the absorption is being calculated,

E = electric field intensity.

P_{abs} is then integrated along spatial coordinates in order to find the total absorption with respect to frequency in the structure. The calculation of total absorption spectrum is very significant as it provides the resonance shifts and hence the sensitivity performance for different protein samples.

Chapter-6

SIMULATION AND RESULT ANALYSIS

6.1) Physical Parameter Variation

We know aspect ratio, R = L / W

Where L = length of the gold nanorod,

W = width of the gold nanorod.

From Gans Theory (equation 7), it is clear that absorption coefficient, σ_{abs} increases with R. As σ_{abs} increases the corresponding SPR Shift also increases with R. So, we evaluated different values of SPR Shift with increasing L (for gold nanorod) with respect to the frequency of light and investigated this proportional relationship with Lumerical FDTD simulation. Corresponding SPR Shift vs length of gold nanorod (L) Graph is illustrated in figure-3.

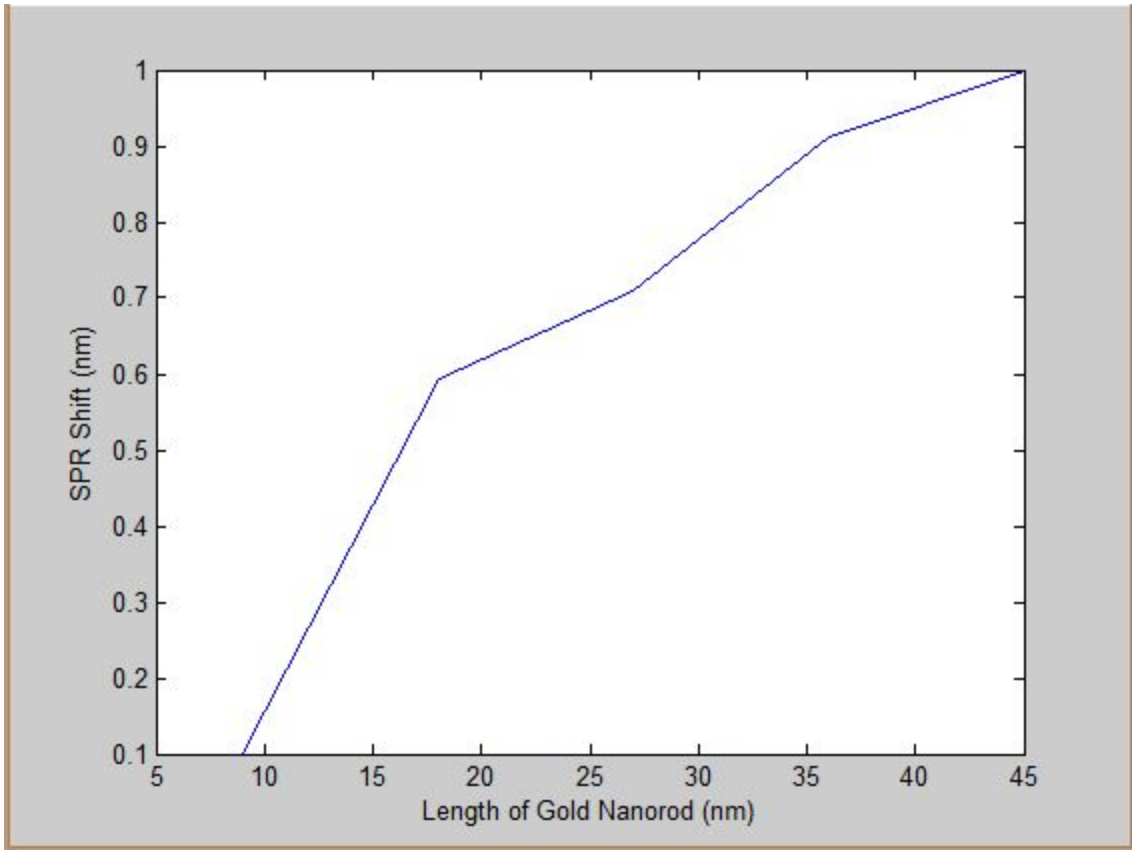

Fig.3. SPR Shift vs Length of Gold Nanorod.

In the same way, SPR Shift will decrease with increasing W. We also investigated this inverse proportional relationship. Corresponding SPR Shift vs width of gold nanorod (W) Graph is illustrated in figure-4.

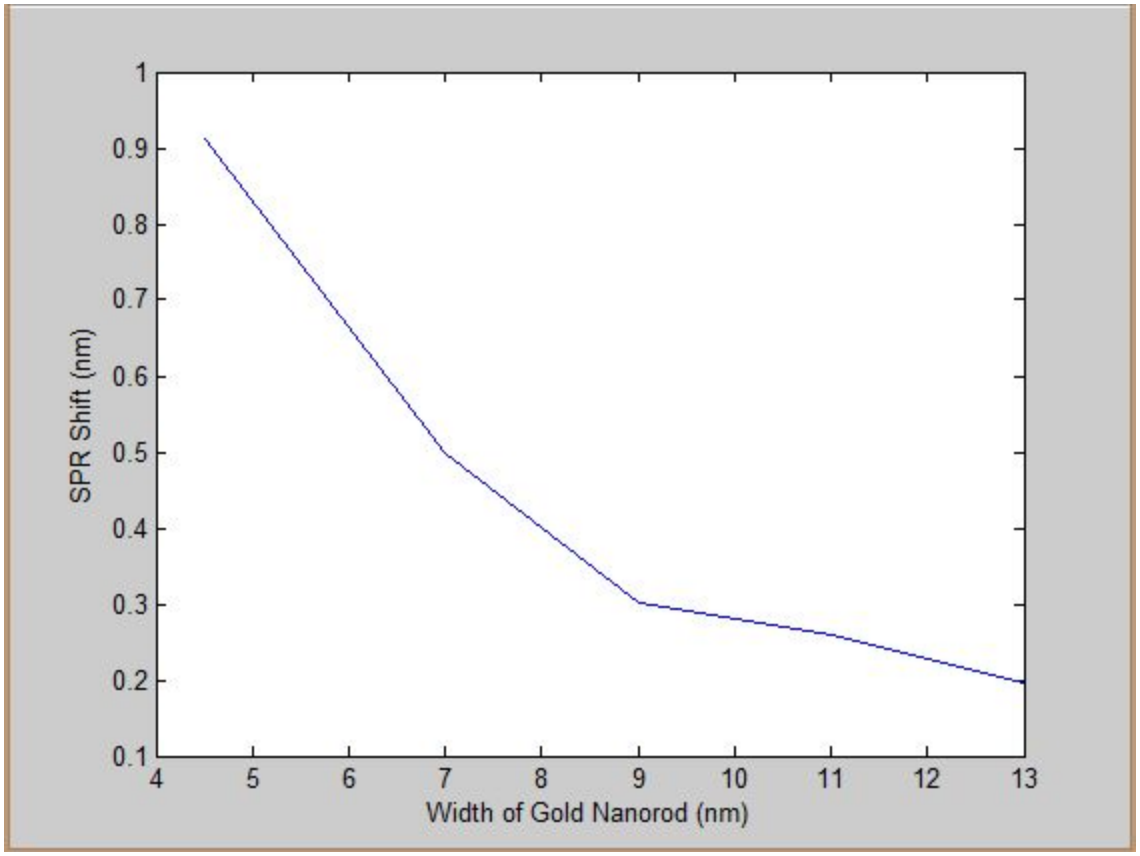

Fig.4. SPR Shift vs Width of Gold Nanorod.

6.2) Physical Environment Variation

6.2.1) Biomolecules' size variation

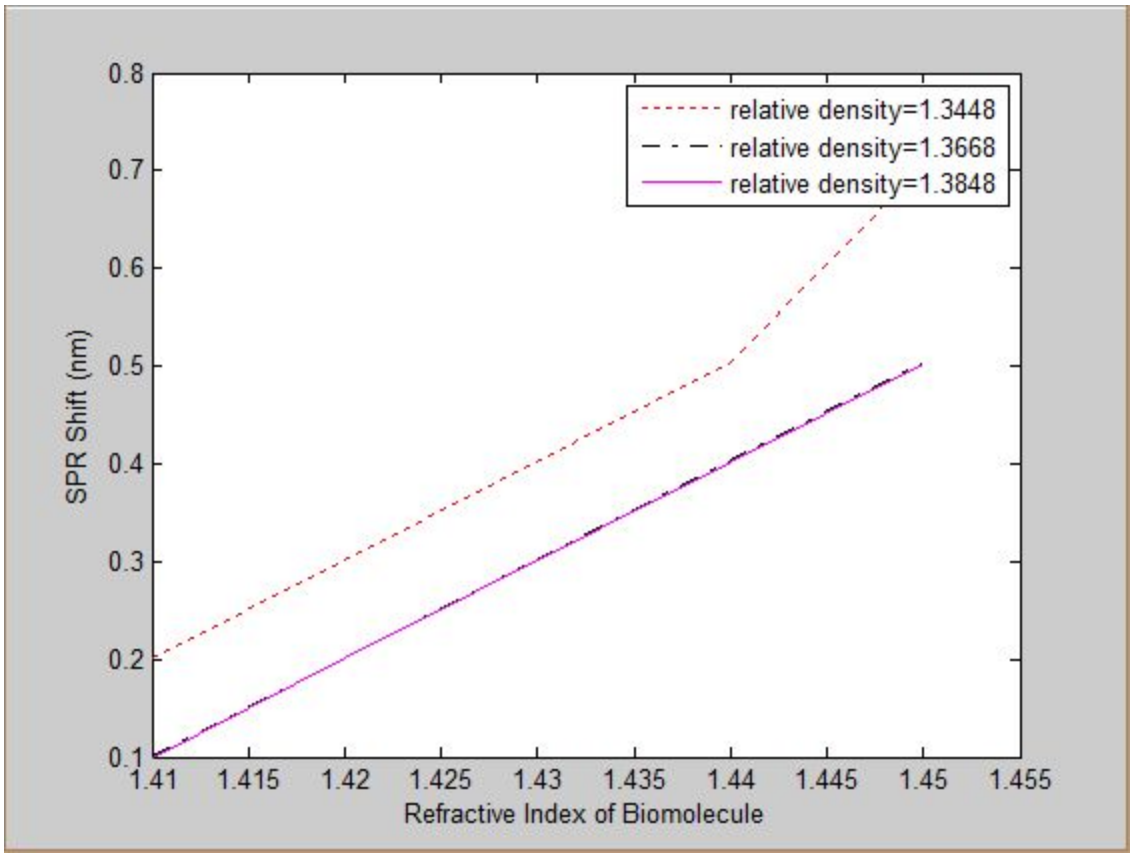

Fig.5. SPR Shift vs Refractive Index of Biomolecule with Relative Density = 1.3448, 1.3668, and 1.3848 (different chaotropic agents)

6.2.2) Substrate Variation

We investigated the SPR Shift by varying substrates via Lumerical FDTD Simulation and observed that SPR Shift is higher for Hydrophobic substrates rather than Hydrophilic substrates.

For example, we got our SPR peak at 822.651 nm frequency for SiO_2 (Hydrophilic substrate) without biomolecule and got our 2nd SPR peak at 823.562 nm frequency with biomolecule. So, the SPR Shift is 0.911 nm. On the other hand, we got 1.109 nm SPR Shift for *Teflon* (Hydrophobic substrate) in the same way.

6.3) Sensitivity of Different Biomolecule

We calculated the SPR Shifts of different protein molecules of different dimensions and refractive indices.

Observed sizes, shapes, refractive indices, and SPR Shifts are shown in the following table:

Protein	**Dimension inside mesh area (nm)**	**Refractive Index**	**SPR Shift (nm)**
HSA	$8 \times 7 \times 4$	1.45	0.607
Fb	$12 \times 3 \times 6$	1.39	0.405
APC	$4.8 \times 4.5 \times 4.3$	1.46	0.303
IgG	$4 \times 3.6 \times 3$	1.42	0.101
Lys	$1.9 \times 1.9 \times 1.9$	1.495	0.303

From our investigation it is clear that SPR Shift increases with the size inside the mesh area and also with refractive index.

HSA has larger dimensions and refractive index than Fb and so SPR Shift is higher for HSA than Fb. In case of APC, though it has higher refractive index than Fb, its dimensions are too low compared with Fb. That's why its SPR Shift is lower than Fb. IgG has lower dimensions and

refractive index compared to APC and so its SPR Shift is lower than APC. Then although Lys has lower dimensions than APC, it has very high refractive index compared to APC and so the SPR Shift is higher than APC.

Chapter-7
CONCLUSION AND FUTURE WORK

With a couple of mechanical upgrades, LSPR sensors could turn into a biomolecular inquire about apparatus on a standard with commercial SPR instruments. As a result of the more noteworthy straightforwardness and lower cost of LSPR, one could consider it "SPR in a cuvette". However sensitivity is needed for LSPR sensors to become a viable benchtop instrument. The single-particle, single-molecule measurements are maximally sensitive and useful for studying the dynamics of single molecules but they are not practical for SPR-like applications. So, scientists must concentrate on enhancing the sensitivity of robust, nanoparticle-ensemble-based substrates.

Another challenge that must be met before LSPR detection can turn into a commercial instrument is to accomplish a more noteworthy vigorousness of the LSPR substrates and consistency among substrates, so that analyte discovery is is not only specific and sensitive, but also reproducible in terms of

LSPR peak wavelength and shift magnitude from substrate to substrate and experiment to experiment. Furthermore, LSPR sensors should have the capacity to distinguish analytes in complex arrangements, that is, biological samples such as blood, serum, urine, and so forth. This is a challenge both in terms of specificity of the sensor and a design that will allow for solutions that are not optically transparent. Glass substrates utilized as a part of a reflection geometry might be most appropriate for this case.

There has been great interest in the potential of LSPR sensing as a fast, simple, low cost medical diagnostic technology. Because LSPR sensing is based on a simple optical extinction measurement, it is conceivable that robust, portable devices for point-of- care diagnostics could be developed and deployed in global outreach programs.

Future difficulties in the improvement of low-cost LSPR-based medical diagnostics may incorporate outlining substrates with greater molecular detection sensitivity, making instruments that

can distinguish target molecules in complex fluids, further miniaturizing the devices, and engineering user-friendly interfaces, in terms of both hardware and software. The perfect substrate would be reusable, simple to functionalize with the recognition element, and simple to clean and replace.

References

[1] Rayleigh, L. (1871). Scientific papers 8 and 9. Philos Mag, 41(107), 274.

[2] Rayleigh, L. (1899). XXXIV. On the transmission of light through an atmosphere containing small particles in suspension, and on the origin of the blue of the sky. The London, Edinburgh, and Dublin Philosophical Magazine and Journal of Science, 47(287), 375-384.

[3] Mie, G. (1908). Beiträge zur Optik trüber Medien, speziell kolloidaler Metallösungen. Annalen der physik, 330(3), 377-445.

[4] Gans, R. (1912). Über die form ultramikroskopischer goldteilchen. Annalen der Physik, 342(5), 881-900.

[5] Minsky, M. (1957). Microscopy apparatus US Patent no. 3013467.

[6] Verellen, N., Sonnefraud, Y., Sobhani, H., Hao, F., Moshchalkov, V. V., Dorpe, P. V., ... & Maier, S. A. (2009). Fano resonances in individual coherent plasmonic nanocavities.

Nano letters, 9(4), 1663-1667.

[7] Mock, J. J., Barbic, M., Smith, D. R., Schultz, D. A., & Schultz, S. (2002). Shape effects in plasmon resonance of individual colloidal silver nanoparticles. The Journal of Chemical Physics, 116(15), 6755-6759.

[8] Fischer, U. C., & Zingsheim, H. P. (1982). Submicroscopic contact imaging with visible light by energy transfer. Applied Physics Letters, 40(3), 195-197.

[9] Pohl, D. W., Denk, W., & Lanz, M. (1984). Optical stethoscopy: Image recording with resolution λ/20. Applied physics letters, 44(7), 651-653.

[10] Klar, T., Perner, M., Grosse, S., Von Plessen, G., Spirkl, W., & Feldmann, J. (1998). Surface-plasmon resonances in single metallic nanoparticles. Physical Review Letters, 80(19), 4249.

[11] Mikhailovsky, A. A., Petruska, M. A., Stockman, M. I., & Klimov, V. I. (2003). Broadband near-field interference spectroscopy of metal nanoparticles using a femtosecond white-light continuum. Optics letters, 28(18), 1686-1688.

[12] Ford, G. W., & Weber, W. H. (1984). Electromagnetic

interactions of molecules with metal surfaces. Physics Reports, 113(4), 195-287.

[13] Barnes, W. L. (1998). Fluorescence near interfaces: the role of photonic mode density. journal of modern optics, 45(4), 661-699.

[14] Barnes, W. L., Dereux, A., & Ebbesen, T. W. (2003). Surface plasmon subwavelength optics. Nature, 424(6950), 824-830.

[15] Maier, S. A., & Atwater, H. A. (2005). Plasmonics: Localization and guiding of electromagnetic energy in metal/dielectric structures. Journal of Applied Physics, 98(1), 011101.

[16] Mühlschlegel, P., Eisler, H. J., Martin, O. J. F., Hecht, B., & Pohl, D. W. (2005). Resonant optical antennas. science, 308(5728), 1607-1609.

[17] Akimov, A. V., Mukherjee, A., Yu, C. L., Chang, D. E., Zibrov, A. S., Hemmer, P. R., ... & Lukin, M. D. (2007). Generation of single optical plasmons in metallic nanowires coupled to quantum dots. Nature, 450(7168), 402-406.

[18] Maier, S. A. (2007). Plasmonics: fundamentals and

applications. Springer Science & Business Media.

[19] Bharadwaj, P., Deutsch, B., & Novotny, L. (2009). Optical antennas. Advances in Optics and Photonics, 1(3), 438-483.

[20] Lakowicz, J. R., & Fu, Y. (2009). Modification of single molecule fluorescence near metallic nanostructures. Laser & Photonics Reviews, 3(1-2), 221-232.

[21] Murray, W. A., & Barnes, W. L. (2007). Plasmonic materials. Advanced materials, 19(22), 3771-3782.

[22] Christopher, P., Xin, H., & Linic, S. (2011). Visible-light-enhanced catalytic oxidation reactions on plasmonic silver nanostructures. Nature chemistry, 3(6), 467-472.

[23] Thimsen, E., Le Formal, F., Grätzel, M., & Warren, S. C. (2010). Influence of plasmonic Au nanoparticles on the photoactivity of Fe2O3 electrodes for water splitting. Nano letters, 11(1), 35-43.

[24] Atwater, H. A., & Polman, A. (2010). Plasmonics for improved photovoltaic devices. Nature materials, 9(3), 205-213.

[25] Le Ru, E., & Etchegoin, P. (2008). Principles of Surface-Enhanced Raman Spectroscopy: and related plasmonic effects. Elsevier.

[26] Mie, G. (1908). Beiträge zur Optik trüber Medien, speziell kolloidaler Metallösungen. *Annalen der physik, 330*(3), 377-445.

[27] Ghosh, S. K., & Pal, T. (2007). Interparticle coupling effect on the surface plasmon resonance of gold nanoparticles: from theory to applications. Chemical reviews, 107(11), 4797-4862.

[28] Schatz, G. C., & Van Duyne, R. P. (2002). Electromagnetic mechanism of surface‐enhanced spectroscopy. Handbook of vibrational spectroscopy.

[29] Maier, S. A., & Atwater, H. A. (2005). Plasmonics: Localization and guiding of electromagnetic energy in metal/dielectric structures. Journal of Applied Physics, 98(1), 011101.

[30] Jones, M. R., Osberg, K. D., Macfarlane, R. J., Langille, M. R., & Mirkin, C. A. (2011). Templated techniques for the synthesis and assembly of plasmonic nanostructures. Chemical Reviews, 111(6), 3736-3827.

[31] Anderson, L. J., Mayer, K. M., Fraleigh, R. D., Yang, Y., Lee, S., & Hafner, J. H. (2010). Quantitative measurements of individual gold nanoparticle scattering cross sections. The Journal of Physical Chemistry C, 114(25), 11127-11132.

[32] Lu, G., Hou, L., Zhang, T., Li, W., Liu, J., Perriat, P., & Gong, Q. (2011). Anisotropic plasmonic sensing of individual or coupled gold nanorods. The Journal of Physical Chemistry C, 115(46), 22877-22885.

[33] Jakab, A., Rosman, C., Khalavka, Y., Becker, J., Trügler, A., Hohenester, U., & Sönnichsen, C. (2011). Highly sensitive plasmonic silver nanorods. ACS nano, 5(9), 6880-6885.

[34] Mannelli, I., & Marco, M. P. (2011). Erratum: Recent advances in analytical and bioanalysis applications of noble metal nanorods. Analytical and Bioanalytical Chemistry, 399(5), 1923-1923.

[35] Le Guével, X., Wang, F. Y., Stranik, O., Nooney, R., Gubala, V., McDonagh, C., & MacCraith, B. D. (2009). Synthesis, stabilization, and functionalization of silver nanoplates for biosensor applications. The Journal of Physical Chemistry C, 113(37), 16380-16386.

[36] Charles, D. E., Gara, M., Aherne, D., Ledwith, D. M., Kelly, J. M., Blau, W. J., & Brennan-Fournet, M. E. (2011). Scaling of surface plasmon resonances in triangular silver

nanoplate sols for enhanced refractive index sensing. Plasmonics, 6(2), 351-362.

[37] Charles, D. E., Aherne, D., Gara, M., Ledwith, D. M., Gun'ko, Y. K., Kelly, J. M., ... & Brennan-Fournet, M. E. (2009). Versatile solution phase triangular silver nanoplates for highly sensitive plasmon resonance sensing. Acs Nano, 4(1), 55-64.

[38] Sweeney, C. M., Stender, C. L., Nehl, C. L., Hasan, W., Shuford, K. L., & Odom, T. W. (2011). Optical properties of tipless gold nanopyramids. Small, 7(14), 2032-2036.

[39] Mayer, K. M., Hao, F., Lee, S., Nordlander, P., & Hafner, J. H. (2010). A single molecule immunoassay by localized surface plasmon resonance. Nanotechnology, 21(25), 255503.

[40] Lee, S., Mayer, K. M., & Hafner, J. H. (2009). Improved localized surface plasmon resonance immunoassay with gold bipyramid substrates. Analytical chemistry, 81(11), 4450-4455.

[41] Kou, X., Sun, Z., Yang, Z., Chen, H., & Wang, J. (2008). Curvature-directed assembly of gold nanocubes, nanobranches, and nanospheres. Langmuir, 25(3), 1692-1698.

[42] Ringe, E., McMahon, J. M., Sohn, K., Cobley, C., Xia, Y., Huang, J., ... & Van Duyne, R. P. (2010). Unraveling the effects of size, composition, and substrate on the localized surface plasmon resonance frequencies of gold and silver nanocubes: a systematic single-particle approach. The Journal of Physical Chemistry C, 114(29), 12511-12516.

[43] Raza, S., Toscano, G., Jauho, A. P., Mortensen, N. A., & Wubs, M. (2013). Refractive-index sensing with ultrathin plasmonic nanotubes. Plasmonics, 8(2), 193-199.

[44] Dondapati, S. K., Sau, T. K., Hrelescu, C., Klar, T. A., Stefani, F. D., & Feldmann, J. (2010). Label-free biosensing based on single gold nanostars as plasmonic transducers. Acs Nano, 4(11), 6318-6322.

[45] Joshi, G. K., McClory, P. J., Dolai, S., & Sardar, R. (2012). Improved localized surface plasmon resonance biosensing sensitivity based on chemically-synthesized gold nanoprisms as plasmonic transducers. Journal of Materials Chemistry, 22(3), 923-931.

[46] Cortie, M. B., & McDonagh, A. M. (2011). Synthesis and optical properties of hybrid and alloy plasmonic nanoparticles. Chemical reviews, 111(6), 3713-3735.

[47] Olson, T. Y., Schwartzberg, A. M., Orme, C. A., Talley, C. E., O'Connell, B., & Zhang, J. Z. (2008). Hollow gold-silver double-shell nanospheres: structure, optical absorption, and surface-enhanced Raman scattering. The Journal of Physical Chemistry C, 112(16), 6319-6329.

[48] Sendroiu, I. E., Warner, M. E., & Corn, R. M. (2009). Fabrication of silica-coated gold nanorods functionalized with

DNA for enhanced surface plasmon resonance imaging biosensing applications. Langmuir, 25(19), 11282-11284.

[49] Cole, J. R., Mirin, N. A., Knight, M. W., Goodrich, G. P., & Halas, N. J. (2009). Photothermal efficiencies of nanoshells and nanorods for clinical therapeutic applications. The Journal of Physical Chemistry C, 113(28), 12090-12094.

[50] Bardhan, R., Mukherjee, S., Mirin, N. A., Levit, S. D., Nordlander, P., & Halas, N. J. (2009). Nanosphere-in-a-nanoshell: a simple nanomatryushka†. The Journal of Physical Chemistry C, 114(16), 7378-7383.

[51] Schladt, T. D., Shukoor, M. I., Schneider, K., Tahir, M. N., Natalio, F., Ament, I., ... & Theato, P. (2010). Au@ MnO nanoflowers: hybrid nanocomposites for selective dual functionalization and imaging. Angewandte Chemie International Edition, 49(23), 3976-3980.

[52] López-Tejeira, F., Paniagua-Domínguez, R., & Sánchez-Gil, J. A. (2012). High-performance nanosensors based on plasmonic Fano-like interference: probing refractive index with individual nanorice and nanobelts. ACS nano, 6(10), 8989-8996.

[53] Guo, L., Yin, Y., Huang, R., Qiu, B., Lin, Z., Yang, H. H., ... & Chen, G. (2012). Enantioselective analysis of melagatran via an lspr biosensor integrated with a microfluidic chip. Lab on a Chip, 12(20), 3901-3906.

[54] Marinakos, S. M., Chen, S., & Chilkoti, A. (2007). Plasmonic detection of a model analyte in serum by a gold nanorod sensor. Analytical chemistry, 79(14), 5278-5283.

[55] Beeram, S. R., & Zamborini, F. P. (2010). Purification of gold nanoplates grown directly on surfaces for enhanced localized surface plasmon resonance biosensing. ACS nano, 4(7), 3633-3646.

[56] Camden, J. P., Dieringer, J. A., Zhao, J., & Van Duyne, R. P. (2008). Controlled plasmonic nanostructures for surface-enhanced spectroscopy and sensing. Accounts of chemical research, 41(12), 1653-1661.

[57] Haynes, C. L., & Van Duyne, R. P. (2001). Nanosphere lithography: a versatile nanofabrication tool for studies of size-dependent nanoparticle optics. The Journal of Physical Chemistry B, 105(24), 5599-5611.

[58] Zhu, S., Du, C., & Fu, Y. (2009). Fabrication and characterization of rhombic silver nanoparticles for biosensing. Optical Materials, 31(6), 769-774.

[59] Fredriksson, H., Alaverdyan, Y., Dmitriev, A., Langhammer, C., Sutherland, D. S., Zäch, M., & Kasemo, B. (2007). Hole–mask colloidal lithography. Advanced Materials, 19(23), 4297-4302.

[60] Lucas, B. D., Kim, J. S., Chin, C., & Guo, L. J. (2008). Nanoimprint Lithography Based Approach for the Fabrication of Large‐Area, Uniformly‐Oriented Plasmonic Arrays. Advanced Materials, 20(6), 1129-1134.

[61] Henzie, J., Lee, J., Lee, M. H., Hasan, W., & Odom, T. W. (2009). Nanofabrication of plasmonic structures*. Annual review of physical chemistry, 60, 147-165.

[62] Lee, M. H., Huntington, M. D., Zhou, W., Yang, J. C., & Odom, T. W. (2010). Programmable soft lithography: solvent-assisted nanoscale embossing. Nano letters, 11(2), 311-315.

[63] McPhillips, J., McClatchey, C., Kelly, T., Murphy, A., Jonsson, M. P., Wurtz, G. A., ... & Pollard, R. J. (2011). Plasmonic sensing using nanodome arrays fabricated by soft nanoimprint lithography. The Journal of Physical Chemistry C, 115(31), 15234-15239.

[64] Cattoni, A., Ghenuche, P., Haghiri-Gosnet, A. M., Decanini, D., Chen, J., Pelouard, J. L., & Collin, S. (2011). λ3/1000 plasmonic nanocavities for biosensing fabricated by soft UV nanoimprint lithography. Nano letters, 11(9), 3557-3563.

[65] Im, H., Lee, S. H., Wittenberg, N. J., Johnson, T. W., Lindquist, N. C., Nagpal, P., ... & Oh, S. H. (2011). Template-stripped smooth Ag nanohole arrays with silica shells for surface plasmon resonance biosensing. ACS nano, 5(8), 6244-6253.

[66] Liang, C. C., Liao, M. Y., Chen, W. Y., Cheng, T. C., Chang, W. H., & Lin, C. H. (2011). Plasmonic metallic nanostructures by direct nanoimprinting of gold nanoparticles. Optics express, 19(5), 4768-4776.

[67] Lee, S. W., Lee, K. S., Ahn, J., Lee, J. J., Kim, M. G., & Shin, Y. B. (2011). Highly sensitive biosensing using arrays of

plasmonic Au nanodisks realized by nanoimprint lithography. ACS nano, 5(2), 897-904.

[68] Lee, S. H., Cho, B., Yoon, S., Jeong, H., Jon, S., Jung, G. Y., ... & Kim, W. B. (2011). Printing of sub-100-nm metal nanodot arrays by carbon nanopost stamps. ACS nano, 5(7), 5543-5551.

[69] Lee, M. H., Lin, J. Y., & Odom, T. W. (2010). Large‐Area Nanocontact Printing with Metallic Nanostencil Masks. Angewandte Chemie, 122(17), 3121-3124.

[70] Vazquez-Mena, O., Gross, L., Xie, S., Villanueva, L. G., & Brugger, J. (2015). Resistless nanofabrication by stencil lithography: A review. Microelectronic Engineering, 132, 236-254.

[71] Aksu, S., Yanik, A. A., Adato, R., Artar, A., Huang, M., & Altug, H. (2010). High-throughput nanofabrication of infrared

plasmonic nanoantenna arrays for vibrational nanospectroscopy. Nano letters, 10(7), 2511-2518.

[72] Vazquez-Mena, O., Sannomiya, T., Tosun, M., Villanueva, L. G., Savu, V., Voros, J., & Brugger, J. (2012). High-resolution resistless nanopatterning on polymer and flexible substrates for plasmonic biosensing using stencil masks. Acs Nano, 6(6), 5474-5481.

[73] Aksu, S., Huang, M., Artar, A., Yanik, A. A., Selvarasah, S., Dokmeci, M. R., & Altug, H. (2011). Flexible plasmonics on unconventional and nonplanar substrates. Advanced Materials, 23(38), 4422-4430.

[74] Kabashin, A. V., Evans, P., Pastkovsky, S., Hendren, W., Wurtz, G. A., Atkinson, R., ... & Zayats, A. V. (2009). Plasmonic nanorod metamaterials for biosensing. Nature materials, 8(11), 867-871.

[75] McPhillips, J., Murphy, A., Jonsson, M. P., Hendren, W. R., Atkinson, R., Höök, F., ... & Pollard, R. J. (2010). High-performance biosensing using arrays of plasmonic nanotubes. ACS nano, 4(4), 2210-2216.

[76] Chang, T. Y., Huang, M., Yanik, A. A., Tsai, H. Y., Shi, P., Aksu, S., ... & Altug, H. (2011). Large-scale plasmonic microarrays for label-free high-throughput screening. Lab on a Chip, 11(21), 3596-3602.

[77] Yan, B., Boriskina, S. V., & Reinhard, B. M. (2011). Design and implementation of noble metal nanoparticle cluster arrays for plasmon enhanced biosensing. The Journal of Physical Chemistry C, 115(50), 24437-24453.

[78] Le Guével, X., Wang, F. Y., Stranik, O., Nooney, R., Gubala, V., McDonagh, C., & MacCraith, B. D. (2009). Synthesis, stabilization, and functionalization of silver nanoplates for biosensor applications. The Journal of Physical Chemistry C, 113(37), 16380-16386.

[79] Lee, S., Mayer, K. M., & Hafner, J. H. (2009). Improved localized surface plasmon resonance immunoassay with gold bipyramid substrates. Analytical chemistry, 81(11), 4450-4455.

[80] Dondapati, S. K., Sau, T. K., Hrelescu, C., Klar, T. A., Stefani, F. D., & Feldmann, J. (2010). Label-free biosensing based on single gold nanostars as plasmonic transducers. Acs Nano, 4(11), 6318-6322.

[81] Valsecchi, C., & Brolo, A. G. (2013). Periodic metallic nanostructures as plasmonic chemical sensors. Langmuir, 29(19), 5638-5649.

[82] Beeram, S. R., & Zamborini, F. P. (2010). Purification of gold nanoplates grown directly on surfaces for enhanced localized surface plasmon resonance biosensing. ACS nano, 4(7), 3633-3646.

[83] Gans, R. (1912). Über die form ultramikroskopischer goldteilchen. Annalen der Physik, 342(5), 881-900.

[84] Le Ru, E., & Etchegoin, P. (2008). Principles of Surface-Enhanced Raman Spectroscopy: and related plasmonic effects. Elsevier.

[85] Johnson, P. B., & Christy, R. W. (1972). Optical constants of the noble metals. Physical review B, 6(12), 4370.